Journal of Magnetism and Magnetic Materials 395 (2015) 73–80

Contents lists available at ScienceDirect

Journal of Magnetism and Magnetic Materials

journal homepage: www.elsevier.com/locate/jmmm

Phase and magnetic properties evolutions of $Y_{3-x}(CaZr)_xFe_{5-x}O_{12}$ by the sol–gel method

Lili Wang [a,b,*], Zhigao Huang [a,b], Huiqin Zhang [a], Ruibing Yu [a]

[a] College of Physics and Energy, Fujian Normal University, Fuzhou 350117, China
[b] Fujian Provincial Key Laboratory of Quantum Manipulation and New Energy Materials, Fuzhou 350117, China

ARTICLE INFO

Article history:
Received 12 May 2015
Received in revised form
27 June 2015
Accepted 12 July 2015
Available online 14 July 2015

Keywords:
YIG
Sol–gel method
Zr-substitution
Magnetic property

ABSTRACT

In this work, $Y_{3-x}(CaZr)_xFe_{5-x}O_{12}$ ($(CaZr)_x$:YIG) were prepared by the sol–gel method. High substituted $(CaZr)_x$:YIG nanoparticles with x up to 0.7 were obtained at 1080 °C, below the melting point of Cu electrode. The average sizes calculated by Scherrer formula decreased from 92.4 nm to 70.0 nm when the substitution amount increased from 0 to 0.7, which was consistent with the results of TEM. The sintering temperature required to form pure garnet phase increased from 690 °C to 1065 °C as the substitution amount x increased from 0 to 0.7 for probable homogeneity destruction by Ca^{2+} and Zr^{4+}. The maximum saturation magnetization (M_s) of 29.8 emu/g was achieved at $x=0.3$. The enhancement of M_s was attributed to the quantity reduction of Fe^{3+} in a-site and the increase of net magnetic moment. The observed decline in M_s for the samples with $x>0.3$ might be attributed to the weakness of super-exchange interaction by changing the angle and length of Fe–O–Fe bonds too much. The complex variations of the coecivities (H_c) indicated the crystal structure from single domain to multiple domains as the sintering temperature increased. Comparing the properties of the samples with $x=0$ and 0.3, it seemed that the substitution had the influence not only on the formation temperature, but also on the critical size of single domain and the temperature of the critical size emerging.

1. Introduction

Yttrium iron garnet (YIG, $Y_3Fe_5O_{12}$) materials are interesting ferromagnetic materials because of their good soft-magnetic properties and high resistivity, and show potential application in microwave devices such as phase shifter, isolator, circulator and antenna [1]. YIG is cubic structure (space group *Ia3d*), in which O^{2-} is closed-packing arrangement, and the cations fill in the interspace of O^{2-} forming three sub-lattices: dodecahedron, octahedron and tetrahedron. The ion distribution structure can be represented by writing the formula as $\{Y_3\}[Fe_2](Fe_3)O_{12}$, { }, [ ], ( ) representing 24*c* (dodecahedral, *c* site), 16*a* (octahedral, *a* site) and 24*d* (tetrahedral, *d* site), respectively. Y^{3+} has relatively large ion radius (0.892 Å), and occupies the interspace of dodecahedron. Fe^{3+} occupies the interspaces of dodecahedron and tetrahedron with ion radius of 0.642 Å and 0.492 Å respectively. Y^{3+} in *c* site has very tiny magnetic moment, the molecule magnetic moment of YIG mainly derive from Fe^{3+} in a site and *d* site. The directions of magnetic moment in a site and *d* site are opposite, and they form anti-ferromagnetic super exchange coupling through oxygen ions. So YIG shows the characteristic of ferrimagnetism. The direction of total magnetic moment is as the same as that of *d* site.

As is well known, the conventional solid state reaction method for preparation of YIG powders from oxides often requires prolonged grinding and high temperature calcinations (usually above 1300 °C), and yields large particles with broad size distribution [2–5]. $YFeO_3$ and Fe_2O_3 are produced as intermediates and these phases remain as impurities unless heated to high temperatures. Co-sintering of ferromagnetic materials with electrodes plays a key role in the integration of microwave devices. However, the sintering temperature of YIG is far beyond the melting points of most electrodes, for example 961 °C for Ag, 1063 °C for Au, 1083 °C for Cu and 1145 °C for Ag–Pd. To overcome these troubles, various wet-chemical methods have been used to synthesize finer and more homogenous YIG powders, such as chemical co-precipitation [6–8], sol–gel method [9–12], sol–gel combustion [13–15]. Among them, the sol–gel method has attracted much attention due to the finer and more homogeneous particles produced. Moreover, the molecular level mixing and the tendency of partially hydrolyzed species to form extended networks facilitate the structure evolution thereby lowering the crystallization temperature.

It is well known that the properties of YIG can change significantly depending on the nature and amount of ion substitution

* Corresponding author at: College of Physics and Energy, Fujian Normal University, Fuzhou 350117, China Fax: +86 591 86397383.
E-mail address: llwang@fjnu.edu.cn (L. Wang).

http://dx.doi.org/10.1016/j.jmmm.2015.07.025
0304-8853/

and the synthesis conditions. The sol–gel method is also convenient to prepare substituted YIG. For example, replacing Y^{3+} ion with rare earth ions such as La^{3+} [16], Ce^{3+} [17], Nd^{3+} [18], Dy^{3+} [19], Er^{3+} [20] can adjust the M_s. Replacing Y^{3+} ion with Gd^{3+} [8,21] can adjust the M_s and improve temperature stability. Also mixed substitutions [22, 23] can adjust the magnetic properties of YIG. The properties of YIG can also be adjusted by replacing Fe^{3+} ions in a site and *d* site with other magnetic ions such as Cr^{3+} [24], or non-magnetic ions such as Al^{3+} [25], and so on. The M_s of YIG is relatively low among the magnetic materials. Previous researches have shown that the M_s of YIG could be enhanced by indium (In^{3+}) substitution with the conventional solid state reaction method [26], and later zirconium (Zr^{4+}) was proved to have the similar effect with less cost [27]. Calcium (Ca^{2+}) added for electrostatic balance replaced part of yttrium (Y^{3+}), which further reduced the cost of YIG. In this study, we focus on $(CaZr)_x$:YIG materials using the sol–gel method. A systematic study of the sol–gel technique for the synthesis of YIG has been presented by Vaqueiro [28], and the results showed that citric acid was a suitable chelating agent to obtain the fine YIG particles. So citric acid was chosen in the course of preparation. The influence of CaZr substitution on the phase formations and the microstructures was investigated. The magnetic properties of $(CaZr)_x$:YIG with different substitution amount and sintering temperatures were systematically studied.

2. Experimental

All the starting materials were analytical purity grade, and used without further .The $(CaZr)_x$:YIG ($x=0$, 0.1, 0.2, 0.3, 0.4, 0.5, 0.6, 0.7) samples were prepared by the sol–gel method. A sol was obtained from an aqueous solution of citric acid mixed with iron (III) nitrate, yttrium nitrate, calcium nitrate and zirconium nitrate. For example, the sol of YIG without substitution ($Y_3Fe_5O_{12}$) was prepared as followed: 9 mmol yttrium nitrate and 15 mmol iron (III) nitrate were dissolved in 50 mL 2 mol/L citric acid solution. $NH_3 \cdot H_2O$ was added to adjust pH value to 2 under stirring to form the sol. Then the sol was put into an oven, and heated at 105 °C for 24 h to form the gel. The gel was then dried at 125 °C for 24 h, and further dried at 140 °C for 12 h to form the xerogel, which was ground into powder after cooling down to room temperature. After heated at 450 °C for 2 h to decompose citrate acid, a part of the powder was mixed with polyvinyl alcohol glue, and pressed into thin disks. Sintering treatments were performed in air at different temperatures (between 680 °C and 1150 °C) for 2 h. The heating and cooling rates were kept at 3 °C per min. The process for the samples sintered at 1080 °C was carried out as Fig. 1 for example. For the substituted samples, the materials amount was adjusted along with *x* value, and the processes were the same as $Y_3Fe_5O_{12}$ sample.

Phase composition and crystal structure were identified by X-ray diffraction (Y2000) using Cu-Kα radiation ($\lambda=1.5406$ Å). The XRD patterns were registered in a 2θ range of 15–80° with a step size of 0.02°. Transmission electron microscopy (JOEL-2100F) was employed to characterize the particle shapes and sizes of the sintered samples. In addition, magnetic properties were measured on a vibrating sample magnetometer (VSM-verslab). The crystallite sizes were calculated using Scherrer's formula: $D \cdot \lambda \cdot k = B \cdot \cos 2\theta$ where '*D*' was the average diameter of crystallites in nm; '*k*' was the shape factor 0.89; '*B*' was the broadening of the diffraction line measured half of its maximum intensity in 'radians'; 'λ' was the wave length of X-ray and '2θ' is the Bragg's diffraction angle. The crystallite sizes of the samples were estimated from the line width of the (420) XRD peaks.

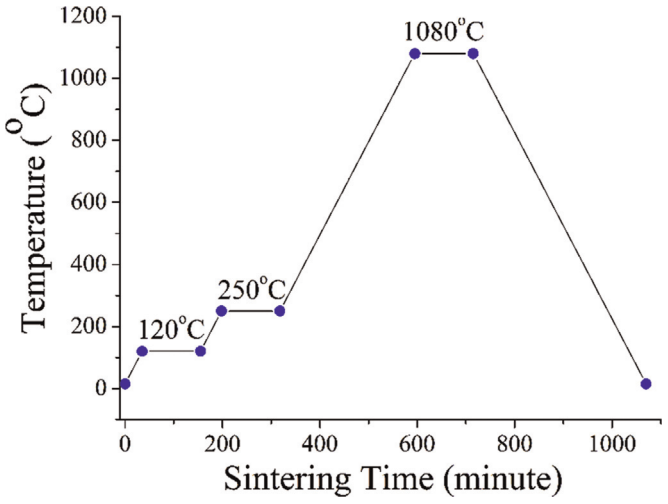

Fig. 1. The process for sample sintered at 1080 °C.

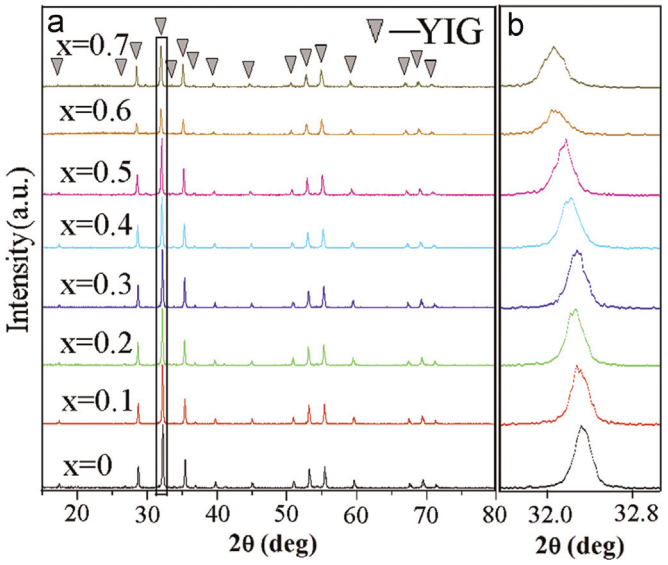

Fig. 2. (a) XRD patterns of $(CaZr)_x$:YIG ferrites sintered at 1080 °C; (b) the enlargements of (420) peaks.

3. Results and discussions

Fig. 2a shows the XRD patterns of $(CaZr)_x$:YIG ferrites sintered at 1080 °C. The pattern at the bottom of Fig. 2a corresponds to the non-substituted sample ($x=0$). Some obvious peaks appear in the pattern among 15°–80° 2θ value, that is 17.54°, 26.93°, 28.82°, 32.31°, 33.91°, 35.49°, 36.99°, 39.84°, 45.10°, 51.07°, 53.30°, 55.49°, 59.69°, 67.62°, 69.53° and 71.42°. The positions and relative intensities of these peaks are consistent with standard garnet YIG pattern (JCPDs 43-0507), which implies that the non-substituted sample is YIG. The average crystal size of the non-substituted YIG is 92.4 nm calculated from Scherrer formula (Table 1). The XRD patterns of $(CaZr)_x$:YIG samples ($x=0.1$–0.7) are also presented in Fig. 2a upper the non-substituted sample. It is clear that all the substituted samples have the same pattern as YIG phase without any impurity appearance, which implies that Ca^{2+} and Zr^{4+} substitutions does not change the crystal type. Fig. 2b shows the enlargements of the strongest (420) peaks. The strongest peaks shift toward the lower angles with increasing CaZr amount, which can also be found for other peaks. Moreover, as shown in Fig. 3, their cell parameters obtained through a fitting analysis of the XRD pattern using software Jade5 demonstrate a nearly linear increase

Table 1
Magnetic parameters and crystal sizes of the samples sintered at 1080 °C with different x values.

Parameters	x Values							
	0	0.1	0.2	0.3	0.4	0.5	0.6	0.7
M_s (emu/g)	25.1	27.3	29.0	29.8	27.3	24.5	21.5	20.8
H_c (Oe)	9.0	40.5	47.5	49.0	22.5	17.0	19.5	13.0
M_r (emu/g)	1.2	7.6	8.1	8.2	2.1	1.7	0.9	0.8
D (nm)	92.4	87.7	85.3	85.6	79.1	78.3	72.9	70.0

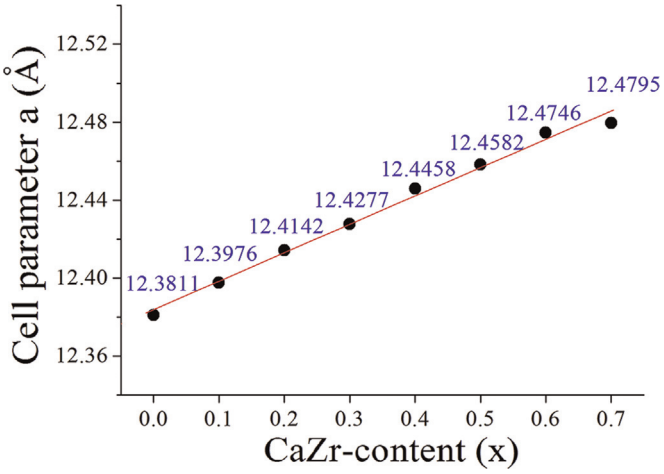

Fig. 3. Variations of the cell parameter for $(CaZr)_x$:YIG ferrites with x=0–0.7.

with increase in the substitution amount. Such an enlargement of crystal cell can be attributed to the replacement of smaller Y^{3+} and Fe^{3+} ions by larger Ca^{2+} and Zr^{4+} ions in the garnet structure in view of the fact that the ionic radii of Y^{3+}, Fe^{3+}, Ca^{2+} and Zr^{4+} are 0.892 Å, 0.642 Å, 0.990 Å and 0.792 Å, respectively. The gradual increase of cell parameters with substituted amount further confirms the entry range of x=0–0.7 strongly suggests that the crystal structures of $(CaZr)_x$:YIG should be affected in a single mode by the substitution of Ca^{2+} and Zr^{4+} ions. Fig. 4 shows the TEM images of $(CaZr)_x$:YIG with different substitution amount (x=0, 0.2

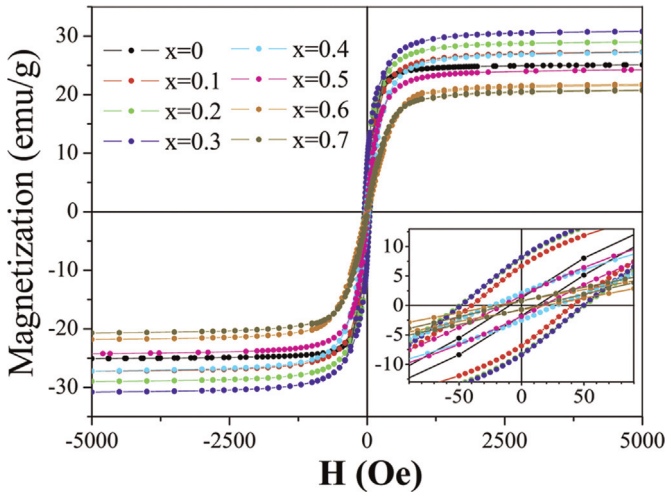

Fig. 5. Room-temperature magnetization curves of the samples with different x values sintered at 1080 °C.

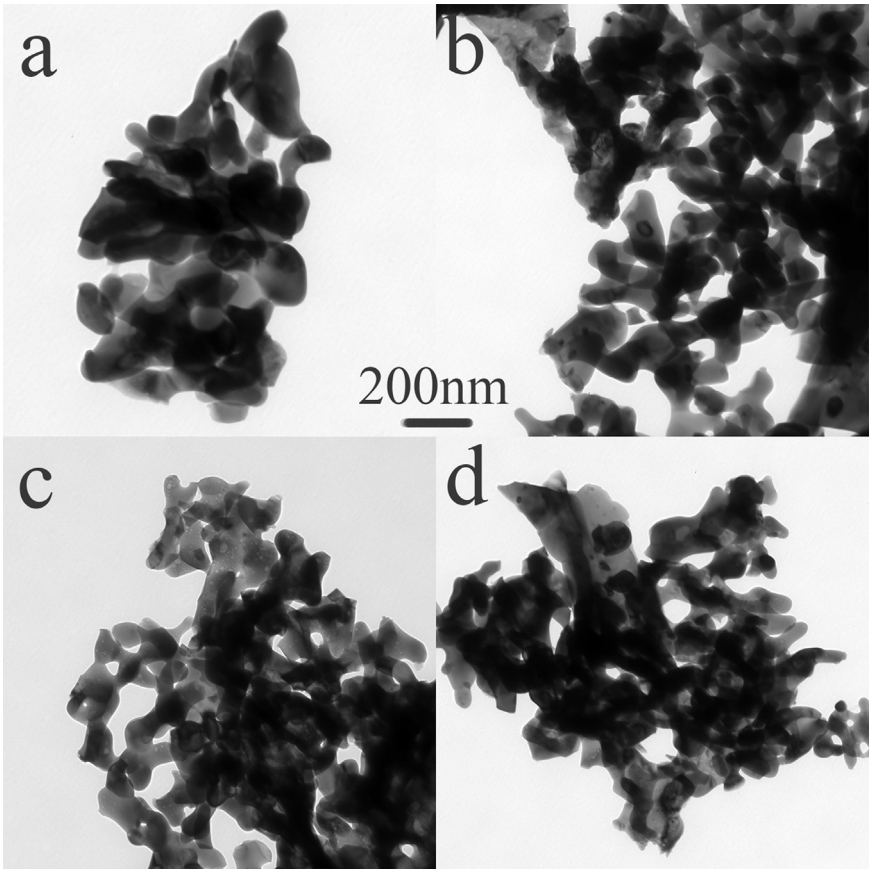

Fig. 4. TEM photos of $(CaZr)_x$:YIG ferrites sintered at 1080 °C. (a) x=0; (b) x=0.2; (c) x=0.4; (d) x=0.6.

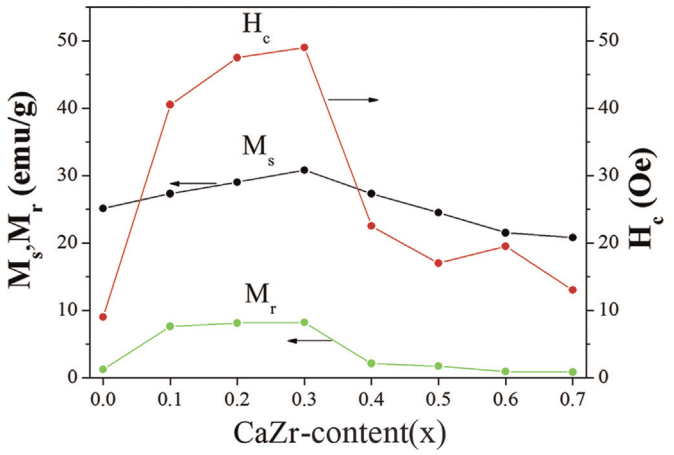

Fig. 6. The variations of M_s, M_r and H_c values of the samples with different x values.

0.4, 0.6) sintered at 1080 °C. Fig. 4a is the photo of the non-substituted sample. Most of the particles from Fig. 4a are around 100 nm, which is consistent with the calculated result from XRD. Meanwhile,it can be seen from the TEM photos that the particle sizes of the substituted samples (Fig. 4(b)–(d)) keep turning smaller as the substitution amount increase, which implies the influence of CaZr substitutions on the particle sizes.

Fig. 5 shows the magnetization curves of the samples sintered at 1080 °C with different x values (x=0–0.7) and the variations of the magnetic parameters are shown in Fig. 6 and Table 1. The M_s of the samples increase with x first, and achieve to the maximum of 29.8 emu/g at x=0.3, then decreased. This result is consistent with the previous research prepared by the conventional solid state reaction method [29]. In view of the fact that the magnetic moments at *a*-, *d*- and *c*- sub-lattices are mutually coupled in antiferromagnetic modes in the YIG-based ferrites. Based on Néel's theory of ferromagnetism in ferrites [22], in $(CaZr)_x$:YIG crystal system, Ca^{2+} and Zr^{4+} are non-magnetic ions, while Y^{3+} and Fe^{3+} are magnetic ions. At room temperature, the three sublattice moments align along the [111] direction. The magnetic moment generated from Y^{3+} is very tiny, so the total magnetic moment can nearly be expressed by formula (1). The direction of the total magnetic moment is the same as that of *d* site. In our samples, Ca^{2+} substituted Y^{3+}, and the main role of Ca^{2+} here was to make charge balance for Zr^{4+} substitution. So Ca^{2+} substitution can fairly affect the total magnetic moment. Zr^{4+} is inclined to occupy a-site, which causes the quantity of Fe^{3+} in a-site reducing and the net magnetic moment increase, thus M_s strengthens [29]. So the M_s is mainly adjusted by Zr^{4+}. As the x value increases, the lattice volume keeps expanding owing to the larger radii of Ca^{2+} and Zr^{4+} (Fig. 3), which will change the angle and length of Fe–O–Fe bonds. If the angle and length of the bonds change too much, the super-exchange interaction will be weakened. So the observed decline in M_s for the samples with $x>0.3$ is attributed to the weakness of super-exchange interaction. The values of the H_c for the samples with different substitution amount fluctuate obviously, and the remanence (M_r) shows the similar behavior. It means that the magnetic properties of the samples with different substitution amount sintered at the same temperature are different from each other. The average particle sizes of the samples calculated by Scherrer formula are also displayed in Table 1. The average sizes decrease from 92.4 nm to 70.0 nm when the substitution amount increase from 0 to 0.7, which is consistent with the results of TEM.

It shows that the properties of the garnet phase are influenced a lot by the substitution from the results above. Therefore, the non-substituted sample and the sample with x=0.3 were selected,

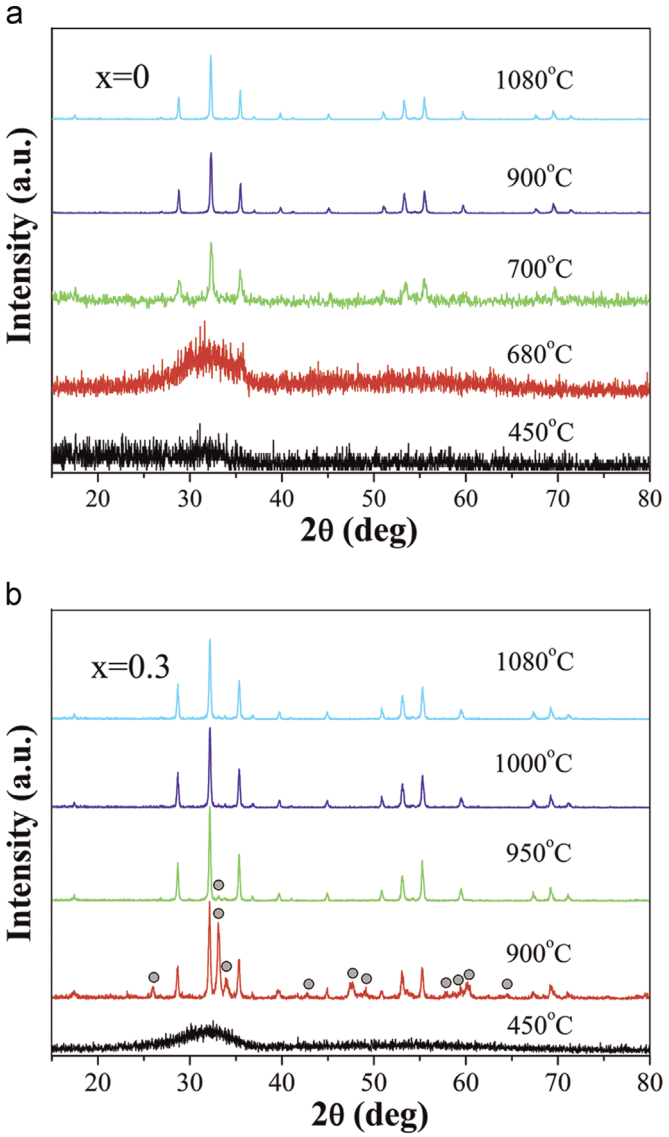

Fig. 7. XRD patterns of $(CaZr)_x$:YIG samples sintered at different temperatures. (a) x=0; (b) x=0.3. The peaks signed with circles belong to $YFeO_3$ phase.

and the structures and properties of them were systematically investigated. First, the phase evolutions of the samples were investigated as a function of sintering temperature from 450 °C to 1080 °C (Fig. 7). The non-substituted sample is mainly amorphous when sintered at 450 °C and 680 °C because only very broad amorphous diffractions appear in the patterns (Fig. 7a). When the temperature rise to 700 °C, the pattern of the sample is consistent with the crystallization of garnet YIG phase (JCPDs43-0507), which implies that garnet phase has already formed. However, the crystallization is not good because the Bragg peaks are still broad. The phase formation temperature of the non-substituted sample must between 680 °C and 700 °C, which isconsistent with the previous research [28]. YIG was formed by a single-step process, where an amorphous precursor powder was formed first and then transformed to YIG during sintering, without any intermediate phase formation [28]. When the temperatures rise to 900 °C and 1080 °C, the patterns are the same as the sample's sintered at 700 °C, except that the Bragg peaks turn to be sharper and narrower indicating the crystallinity enhancement and the crystal size increase. The patterns of the substituted sample with x=0.3 are presented in Fig. 7b. It can be seen that the obvious diffraction peaks of $YFeO_3$ phase (JCPDs 39-1489) present in the pattern of the

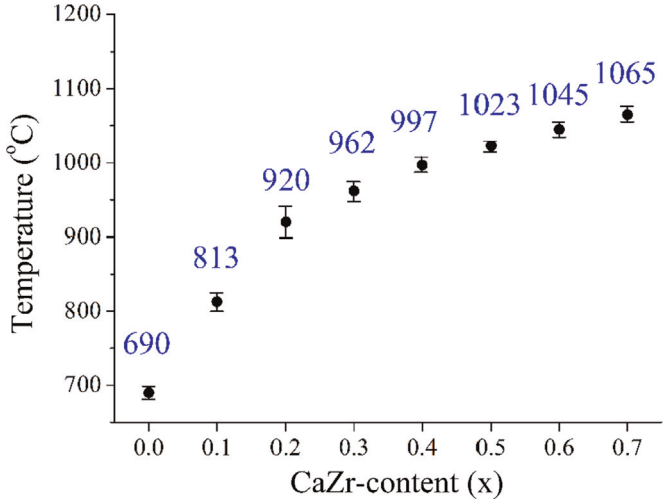

Fig. 8. The phase formation temperature of samples with different x values.

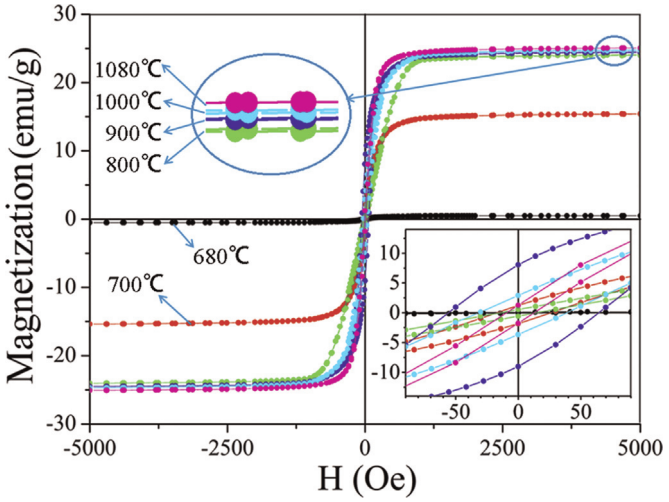

Fig. 9. Room-temperature magnetization curves of the non-substituted samples (x=0) sintered at different temperatures.

sample sintered at 900 °C, which is the intermediate compound in the process of crystallization. So the garnet phase has not completely formed even when the sintering temperature rise to 900 °C. When the temperature further rise to 950 °C, the amount of $YFeO_3$ phase in the sample sharply decreases, but not completely disappears. Pure garnet phase form in the samples sintered at 1000 °C and 1080 °C, and the sharp diffraction peaks indicate the high crystalinity. By the way, the tetragonal YIG phase is not observed in all the samples. It is noticed that the substituted sample with x=0.3 needs the temperature higher than 950 °C to form pure garnet phase, which is much higher than the non-substituted sample. In fact, the phase formation temperatures of the substituted samples are all higher than the non-substituted sample. As shown in Fig. 8, the phase formation temperatures increase from about 690 °C to about 1065 °C as x value increases from 0 to 0.7. The temperature rises more rapidly when x value is lower. It means that higher substitution amount requires higher temperature to form pure garnet phase. The particle sizes are affected by the formation temperature and the substitution amount from the TEM and XRD results. For the lower-substituted sample, the pure phase forms at lower temperature. It means that there is longer time for the particles of lower-substitution sample to grow up. For the higher-substitution sample, the pure phase forms at higher temperature. The impurity phase at the boundaries before the formation of pure YIG phase may hinder the growth of the particles. Therefore, the particle size of higher-substitution sample is smaller. The sample with x=0.8 is not shown here, because the pure garnet phase does not form even if the temperature rises to 1085 °C, which is beyond the melting points of most electrodes, and mostly reaches the melting point of Ag–Pd electrode.

It should be noticed that the formation ways of garnet YIG phase for the non-substituted sample and the substituted samples are different. There is no trace of $YFeO_3$ in the course of YIG formation for the non-substituted sample. The sample is completely amorphous when sintered at 680 °C, then directly changes into garnet YIG phase when the temperature rises to 700 °C without any intermediate phase (Fig. 7a). However, obvious $YFeO_3$ diffraction peaks are observed in the sample with x=0.3 (Fig. 7b). In fact, $YFeO_3$ phase is detected in all substituted samples of our research in the course of the phase formation. The formed phase $YFeO_3$, as often reported in literature, is an inevitable product of poor chemical homogeneity in the precipitates by co-precipitation method [6]. Y^{3+} and Fe^{3+} can homogeneously mix in sol–gel method, so $YFeO_3$ was not detected in the non-substituted sample. However, the mixing state of Y^{3+} and Fe^{3+} may be somewhat

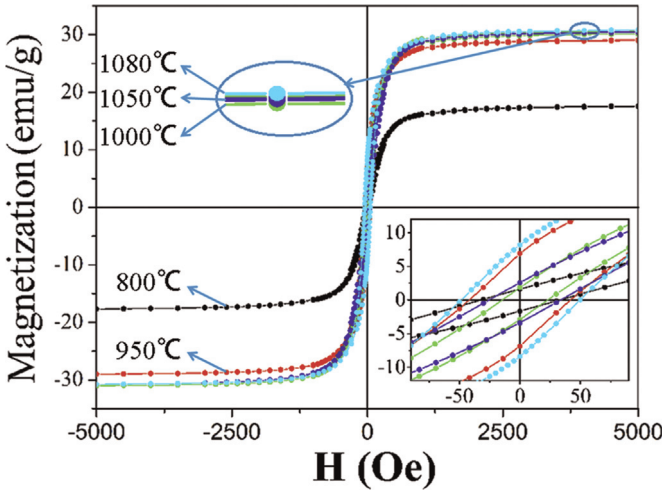

Fig. 10. Room-temperature magnetization curves of the samples with x=0.3 sintered at different temperatures.

destroyed by the addition of Ca^{2+} and Zr^{4+}, which ascribes to the formation of $YFeO_3$. Fortunately, the $YFeO_3$ phase can be eliminated by increasing the temperature. So the substituted samples need higher temperature to form pure garnet phase compared to the non-substituted sample. The larger addition of Ca^{2+} and Zr^{4+} may cause higher extent of inhomogeneity, which results in the higher formation temperature.

Fig. 9 displays the room-temperature magnetization curves of the non-substituted samples (x=0) sintered at different temperatures, and the magnetic parameters are shown in Table 2. It can be seen that the magnetization of the sample sintered at 680 °C is very week, which can be due to the non-crystallization of the sample concluded from the XRD results. As the temperature rises to 700 °C, the M_s of the sample increases to 15.4 emu/g, which is much lower than the M_s of the bulk material (26.8 emu/g). The XRD diffraction peaks of the sample sintered at 700 °C are broad, so it could be concluded that the crystallization of this sample is poor. The low M_s of the sample can be due to the poor crystallization. When the temperature rises to 800 °C, the M_s sharply increased to 24.0 emu/g. As the temperature further rises, the M_s of the samples gradually increase, and reaches to 25.1 emu/g at 1080 °C, which is still lower than the M_s of bulk phase. The XRD diffraction peaks of the samples sintered at the temperatures

Table 2
Magnetic properties and crystal sizes of the samples with $x=0$ and 0.3 sintered at different temperature.

x Values	Parameters	Sintering temperature (°C)								
		700	800	850	900	950	1000	1050	1080	1150
0	M_s (emu/g)	15.4	24.0	24.0	24.4	24.5	24.8	24.8	25.1	25.2
	H_c (Oe)	27.0	13.0	18.0	53.0	56.0	32.0	30.0	9.0	9.0
	M_r (emu/g)	1.3	0.6	1.8	8.1	8.3	3.0	3.2	1.2	1.1
	D (nm)	63.5	–[a]	–	69.1	70.2	73.4	76.0	87.4	93.5
0.3	M_s (emu/g)	–	17.5	–	26.0	28.1	29.1	29.4	29.8	29.9
	H_c (Oe)	–	30.0	–	34.3	41.4	13.8	25.8	49.0	21.2
	M_r (emu/g)	–	1.7	–	2.5	6.2	2.8	3.4	8.8	1.8
	D (nm)	–	–	–	69.0	77.2	79.5	–	85.6	90.5

[a] "–" Means the data here is absent.

higher than 700 °C have already turned sharp, which imply the good crystallization of the samples. So the low M_s must be due to the small nanoparticle sizes of the sample. Fig. 10 displays the room-temperature magnetization curves of the substituted samples with $x=0.3$ sintered at different temperatures, and the magnetic parameters are also shown in Table 2. The M_s of the substituted samples with $x=0.3$ increase with sintering temperature, which is similar to the non-substituted samples. The sample turns to pure garnet-phase around 962 °C, so the M_s of the samples increase evidently below this temperature, and then gradually increase to 29.8 emu/g at 1080 °C.

$$M = \left|M_c - (M_d - M_a)\right| \approx \left|M_d - M_a\right| \quad (1)$$

The H_c and M_r variations of the samples with $x=0$ and 0.3 are not monotonic (Table 2). The variations of H_c can be divided into three regions. For the non-substituted sample, the H_c at 700 °C was 27.0 Oe, which is not a low value. When temperature rises to 800 °C, the H_c sharply decreases to 13.0 Oe, and then increases again. The H_c runs up to the maximum 56.0 Oe at 950 °C, and turns to decrease toward higher temperature. For the sample with $x=0.3$, the H_c keeps increasing from 30.0 Oe at 800 °C to 41.4 Oe at 950 °C, then sharply decreases to 13.8 Oe when temperature rises to 1000 °C. Afterward, the H_c increases again with sintering temperature, and then decreases again. The trends of M_r are similar to their H_c for the two sets of samples. The H_c of the sample with $x=0.3$ undergoes twice rises. The first rise appears below 950 °C, when the pure garner phase does not completely form. The continued increase of H_c below 950 °C can be due to the continual increase amount of magnetic grains. The second rise appears between 1000 °C and 1080 °C, during which the particles keep growing. The magnetic properties of a magnetic material depend largely on the crystal size distributions as the domain structure and magnetization process depends on particle size [30]. When the crystal size is grown to the critical size of single domain, the H_c is decided by magnetic domain rotation, so the H_c reaches the maximum [31]. The H_c of the sample with $x=0.3$ reaches the maximum at 1080 °C, which implies that the crystal size is most near the critical size of single domain, that is 85.6 nm. It can be seen that the H_c of the samples with $x=0.1$ and 0.2 sintered at 1080 °C also exhibit relatively high values (Table 1), which infers that the crystal sizes of these two samples are also near the critical size of single domain of their own. When the crystal size is larger than the critical size of single domain, the H_c is decided by magnetic displacement, so the value of H_c is small. In our research, when the temperature further increases to 1150 °C, the particles grow to 90.5 nm, and the H_c decreases, which indicates that the crystal size has been beyond the critical size of single domain. The higher sintering temperature produces larger crystal size, which makes it easier for magnetic domain walls to move [3]. So the H_c decreases. The non-substituted sample below 700 °C is amorphous, so the H_c cannot be detected. The H_c of the samples sintered between 750 °C and 950 °C keep increasing, which also corresponds to the growth of the crystals with single domain. The H_c reaches a relatively high value of 56.0 Oe at 950 °C with an average crystal size of 70.2 nm. Further increase of the temperature results in the growth of the crystals and the decrease in H_c. These results indicate that the non-substituted samples sintered at and below 950 °C are single domains, and are multiple domains at and beyond 1000 °C.

It can be seen that the maximum H_c appear at different temperatures for the two samples, which indicates that the particle sizes of the two samples reach the critical size of single domain at different temperatures. It can be mainly due to the different pure garnet-phase formation temperatures influenced by the substitution. Meanwhile, the average crystal size of the sample with $x=0.3$ at 1080 °C is larger than that of the non-substituted sample at 950 °C, which indicates that the critical size of single domain for the sample with $x=0.3$ is larger than that of the non-substituted sample. It has been found in the previous research that proper Ca^{2+} and Zr^{4+} ions were beneficial to grain growth [27]. It seems that Ca^{2+} and Zr^{4+} ions are also beneficial to domain growth in our research. We notice that the H_c values of both set of samples around the temperatures of pure garnet phase formation are not low, that is 27.0 Oe for the non-substituted sample at 700 °C and 41.4 Oe for the sample with $x=0.3$ at 950 °C. The H_c both sharply decrease at the moment beyond the temperatures of pure garnet phase formation. The structural disorder of the samples in the course of the formation of pure garnet phase may be the reason for the relatively high H_c of the samples. When the garnet phase formation completes, the order degree of the samples evidently enhanced. Therefore, the H_c sharply decreases. The variations of average crystal sizes for these samples are relatively regular. The average crystal sizes roughly decrease as the x values increase, which may attributed to the gradual increase of the formation temperature with x values. On one hand, as the formations of the pure garnet phase are delayed by the substitution, the particle growths may be also delayed. The delay of crystal growth is more evident with more substitution amount. Therefore, the average crystal sizes decrease with the substitution amount. On the other hand, the excessive doping of Ca^{2+} and Zr^{4+} ions may also cause the decrease in the average grain size [29].

$(CaZr)_x$:YIG prepared by the conventional solid state reaction method have been research in elsewhere [27,29]. Compared with the properties of $(CaZr)_x$:YIG prepared by the conventional solid state reaction method, the properties of $(CaZr)_x$:YIG prepared by the sol–gel method are somewhat different. The M_s of YIG without substitution prepared by the sol–gel method at 1080 °C has been very close to the theoretical value. The M_s of the samples with

$x<0.5$ sintered at 1080 °C are much higher than the samples' prepared by the conventional solid state reaction method at 1350 °C [27], and close to the samples' sintered at 1425 °C[29]. These results indicate that the purities and crystallinities of the samples prepared by the sol–gel method sintered at 1080 °C in this work are of high degrees. The crystal sizes in $(CaZr)_x$:YIG samples prepared by the conventional solid state reaction method are several micrometers. The H_c decreases as x value increases from 0 to 0.3 at 1350 °C and 1425 °C. When CaZr amount further increases ($x>0.3$), a second phase will be yielded, and the variation of the properties including H_c become somewhat irregular. As $(CaZr)_x$:YIG samples in our research are prepared by the sol–gel method at lower temperatures, and the crystals are nanometer size. For example, the average crystal sizes in our research are tens of nanometers for the samples with $x=0$ and 0.3, and the critical sizes of single domain for these samples just fall in this range. Therefore, the variations of the properties with temperature and crystal size are more complex. The average crystal sizes of the samples prepared by the sol–gel method are much smaller than those prepared by the conventional solid state reaction method, which results in the totally higher H_c for the existence of more crystal boundaries. Since the variations of the magnetic properties are complex for the existence of the critical size of single domain, it is especially important to choose a proper temperature to keep away from the critical size. For example, the non-substituted sample shows the best soft magnetic properties at 1080 °C with 25.1 emu/g M_s and 9.0 Oe H_c. The sample with $x=0.3$ shows the best soft magnetic properties at 1000 °C with 30.1 emu/g M_s and 13.8 Oe H_c. The sol–gel method can reduce sintering temperature significantly for the samples with and without substitutions. It is not only means lower temperature needed to obtain the products, but also means more space for temperature changes to obtain higher substitution samples and larger adjustable range for the properties. In this work, $(CaZr)_x$:YIG with 0.7 substitution amount was obtained at 1080 °C, whose temperature was still much lower than the temperature used by the conventional solid state reaction method in Ref. [27].

4. Conclusions

In general, high substituted $(CaZr)_x$:YIG samples with x up to 0.7 could be obtained below the melting point of Cu electrode by the sol–gel method, over 300 °C lower than the samples prepared by the conventional solid state reaction method. The average sizes decreased from 92.4 nm to 70.0 nm when the substitution amount increased from 0 to 0.7, which was consistent with the results of TEM. The sintering temperature required to form the pure garnet phase increased from 690 °C to 1065 °C as the substitution amount x increasing from 0 to 0.7 for homogeneity destruction by Ca^{2+} and Zr^{4+}. The M_s of the samples sintered at 1080 °C increased with x first, then decreased. The enhancement of M_s was attributed to quantity reducing of Fe^{3+} in a-site. The observed decline in M_s for the samples with $x>0.3$ might be attributed to the weakness of super-exchange interaction by changing the angle and length of Fe–O–Fe bonds too much. The properties of the samples with $x=0$ and 0.3 were carefully observed. The variations of the H_c with temperatures and crystal sizes were complex for these two sets of samples. The H_c values of both samples around the temperatures of pure garnet phase formation were relatively high, which might due to the structural disorder in the course of the phase formation. The H_c both sharply decreased at the moment beyond the temperatures of pure garnet phase formation. Then the H_c increased again with the temperature as the crystal size gradually approached the critical size of single domain, and reached to the maximum when the crystal size was the closest to the critical size. Further increasing the temperature resulted in the crystals with larger sizes, and the H_c decreased again. Since the variations of the magnetic properties were complex for the existence of the critical size of single domain, it was important to choose a proper temperature to keep away from the critical size. Comparing the properties of the samples with $x=0$ and 0.3, it seemed that the substitution had the influence not only on the formation temperature, but also on the critical size of single domain and the temperature of the critical size emerging.

Acknowledgments

This report was supported by National Natural Science Foundation of China No. 11374052 and 51202031. This report was also supported by Foundation of Fujian Educational Committee No. JB14029.

References

[1] H.W. Zhang, J. Li, H. Su, T.C. Zhou, Y. Long, Z.L. Zheng, Development and application of ferrite materials for low temperature co-fired ceramic technology, Chin. Phys. B 22 (2013) 117504–117525.
[2] J. Wang, J. Yang, Y. Jin, T. Qiu, Effect of manganese addition on the microstructure and electromagnetic properties of YIG, J. Rare Earths 29 (2011) 562–566.
[3] N. Rodziah, M. Hashim, I.R. Idza, I. Ismayadi, A.N. Hapishah, M.A. Khamirul, Dependence of developing magnetic hysteresis characteristics on stages of evolving microstructure in polycrystalline yttrium iron garnet, Appl. Surf. Sci. 258 (2012) 2679–2685.
[4] K. Bouziane, A. Yousif, H.M. Widatallah, J. Amighian, Site occupancy and magnetic study of Al^{3+} and Cr^{3+} co-substituted Y_3Fe_5O, J. Magn. Magn. Mater. 320 (2008) 2330–2334.
[5] Z. AzadiMotlagh, M. Mozaffari, J. Amighian, Preparation of nano-sized Al-substituted yttrium iron garnets by the mechanochemical method and investigation of their magnetic properties, J. Magn. Magn. Mater. 321 (2009) 1980–1984.
[6] W. Zhang, C. Guo, R. Ji, C. Fang, Y. Zeng, Low-temperature synthesis and microstructure-property study of single-phase yttrium iron garnet (YIG) nanocrystals via a rapid chemical coprecipitation, Mater. Chem. Phys. 125 (2011) 646–651.
[7] S. Hong, Y. Kim, C.G. Kim, The microstructure and magnetic properties of YIG powders synthesized by a coprecipitaion and a sonochemical process, J. Magn. 14 (2009) 165–167.
[8] F.R. Lamastra, A. Bianco, F. Leonardi, G. Montesperelli, F. Nanni, G. Gusmano, High density Gd-substituted yttrium iron garnets by coprecipitation, Mater. Chem. Phys. 107 (2008) 274–280.
[9] C.C. Wang, W.T. Yu, The effect of chelating copolymer additive on the yttrium iron garnet (YIG) nanoparticle formation, Polym. Adv. Technol. 20 (2009) 545–549.
[10] E.J. Donahue, M. Ng, P. Li, A determination of structural evolution during the processing of glycol-based, sol-gel derived ceramics through the study of ferrimagnetic interactions, J. Mater. Res. 22 (2007) 3152–3157.
[11] K. Praveena, S. Srinath, Effect of Gd^{3+} on dielectric and magnetic properties of $Y_3Fe_5O_{12}$, J. Magn. Magn. Mater. 349 (2014) 45–50.
[12] K. Sadhana, S.R. Murthy, K. Praveena, Effect of Sm^{3+} on dielectric and magnetic properties of $Y_3Fe_5O_{12}$ nanoparticles, J. Mater. Sci. – Mater. Electron. 25 (2014) 5130–5136.
[13] S.R. Naik, A.V. Salker, Enhancement in the magnetic moment with Cr^{3+} doping and its effect on the magneto-structural properties of $Ce_{0.1}Y_{2.9}Fe_5O_{12}$, Phys. Chem. Chem. Phys. 14 (2012) 10032–10040.
[14] W. Yang, L. Wang, Y. Ding, Q. Zhang, Narrowing of ferromagnetic resonance linewidth in calcium substituted YIG powders by Zr^{4+}/Sn^{4+} substitution, J. Mater. Sci. – Mater. Electron. 25 (2014) 4517–4523.
[15] S.H. Vajargah, H.R.M. Hosseini, Z.A. Nemati, Preparation and characterization of nanocrystalline misch-metal-substituted yttrium iron garnet powder by the sol–gel combustion process, Int. J. Appl. Ceram. Technol. 5 (2008) 464–468.
[16] Z. Cheng, Y. Cui, H. Yang, Y. Chen, Effect of lanthanum ions on magnetic properties of $Y_3Fe_5O_{12}$ nanoparticles, J. Nanoparticle Res. 11 (2009) 1185–1192.
[17] J.S. Kum, S.J. Kim, I.B. Shim, C.S. Kim, Magnetic properties and Mössbauer studies of $Y_{3-x}Ce_xFe_5O_{12}$ (x=0:00, 0:01, and 0:3) fabricated using a sol–gel method, IEEE Trans. Magn. 39 (2003) 3118–3120.
[18] Z. Cheng, H. Yang, Magnetic properties of Nd-$Y_3Fe_5O_{12}$ nanoparticles, J. Mater. Sci. – Mater. Electron. 18 (2007) 1065–1069.
[19] Z. Cheng, H. Yang, Y. Cui, L. Yu, X. Zhao, S. Feng, Synthesis and magnetic properties of $Y_{3-x}Dy_xFe_5O_{12}$ nanoparticles, J. Magn. Magn. Mater. 308 (2007) 5–9.
[20] R. Shaiboub, N.B. Ibrahim, M. Abdullah, F. Abdulhade, The physical properties

of erbium-doped yttrium iron garnet films prepared by sol–gel method, J. Nanomater. 2012 (524903) (2012) 5.
[21] Z. Cheng, H. Yang, L. Yu, Y. Cui, S. Feng, Preparation and magnetic properties of $Y_3Fe_5O_{12}$ nanoparticles doped with the gadolinium oxide, J. Magn. Magn. Mater. 302 (2006) 259–262.
[22] H. Xu, H. Yang, Magnetic properties of Ce, Dy-substituted yttrium iron garnet ferrite powders fabricated using a sol–gel method, Phys. Status Solidi A 204 (2007) 1203–1209.
[23] H. Xu, H. Yang, W. Xu, S. Feng, Magnetic properties of Ce,Gd-substituted yttrium iron garnet ferrite powders fabricated using a sol–gel method, J. Mater. Process. Technol. 197 (2008) 296–300.
[24] H. Xu, H. Yang, Effect of Chromium on magnetic properties of $Y_{2.9}Ce_{0.1}Fe_{5-x}Cr_xO_{12}$ Nanoparticles, Mater. Manuf. Process. 23 (2008) 10–13.
[25] F.W. Aldbea, N.B. Ibrahim, M. Yahya, Effect of adding aluminum ion on the structural, optical, electrical andmagnetic properties of terbium doped yttrium iron garnetnanoparticles films prepared by sol–gel method, Appl. Surf. Sci. 321 (2014) 150–157.
[26] M. Niyaifar, A. Beitollahi, N. Shiri, M. Mozaffari, J. Amighian, Effect of indium addition on the structure and magnetic properties of YIG, J. Magn. Magn. Mater. 322 (2010) 777–779.
[27] Y.Y. Huang, J. Yang, T. Qiu, J.Q. Wang, Y.L. Jin, Effects of Zr-substitution on microstructure and properties of YCaVIG ferrites, J. Magn. Magn. Mater. 324 (2012) 934–938.
[28] P. Vaqueiro, M.P. Crosnier-Lopez, M.A. López-Quintela, Synthesis and characterization of yttrium iron garnet nanoparticles, J. Solid State Chem. 126 (1996) 161–168.
[29] J. Wang, Y. Jin, J. Yang, Y. Huang, T. Qiu, Effect of ZrO_2 addition on the microstructure and electromagnetic properties of YIG, J. Alloy. Comp. 509 (2011) 5853–5857.
[30] Q.M. Xu, W.B. Liu, L.J. Hao, C.J. Gao, X.G. Lu, Y.A. Wang, J.S. Zhou, Effects of In-substitution on the microstructure and magnetic properties of Bi-CVG ferrite with low temperature sintering, J. Magn. Magn. Mater. 322 (2010) 2276–2280.
[31] C. Guo, W. Zhang, R. Ji, Y. Zeng, Effects of In3+-substitution on the structure and magnetic properties of multi-doped YIG ferri tes with low saturation magnetizations, J. Magn. Magn. Mater. 323 (2011) 611–615.